Fish and Shellfish Immunology 89 (2019) 614–622

Contents lists available at ScienceDirect

Fish and Shellfish Immunology

journal homepage: www.elsevier.com/locate/fsi

Full length article

Characterisation of scavenger receptor class B type 1 in rare minnow (*Gobiocypris rarus*)

Mi Ou[a], Rong Huang[b], Qing Luo[a], Lv Xiong[b], Kunci Chen[a,**], Yaping Wang[b,*]

[a] Key Laboratory of Tropical and Subtropical Fishery Resources Application and Cultivation, Ministry of Agriculture, Pearl River Fisheries Research Institute, Chinese Academy of Fishery Sciences, Guangzhou, 510380, China

[b] State Key Laboratory of Freshwater Ecology and Biotechnology, Institute of Hydrobiology, Chinese Academy of Sciences, Wuhan, 430072, China

ARTICLE INFO

Keywords:
Rare minnow
GCRV
SRB1
Receptor
Cell entry

ABSTRACT

Scavenger receptor class B type 1 (SRB1) is a transmembrane protein belonging to the scavenger receptors (SRs) family and it plays an important role in viral entry. Not much is known on SRB1 in teleost fish. Grass carp reovirus (GCRV) cause huge economic losses in grass carp industry. In this study, rare minnow (*Gobiocypris rarus*) was used as a model fish to investigate the mechanism of GCRV infection, which is sensitive to GCRV. The structure of *SRB1* gene in *G. rarus* (*GrSRB1*) was cloned and elucidated. *GrSRB1* is composed of 13 exons and 12 introns, and its full-length cDNA is 2296 bp in length, with 1521 bp open reading frame (ORF) that encodes a 506 amino acid protein. The *Gr*SRB1 protein is predicted to contain a typical CD36 domain and two transmembrane regions. In *G. rarus*, *GrSRB1* is expressed strongly in the liver (L), intestines (I), brain (B) and muscle (M), while it is expressed poorly in the heart (H), middle kidney (MK), head kidney (HK) and gills (G). After infection with GCRV, *GrSRB1* expression was up-regulated in main immune tissues during the early infection period. Moreover, co-immunoprecipitation assays revealed that *Gr*SRB1 could interact with the outer capsid protein of GCRV (VP5 and VP7). These results suggest that *Gr*SRB1 could be a receptor for GCRV. We have managed to characterize the *GrSRB1* gene and provide evidence for its potential functions for GCRV entry into host cells.

1. Introduction

Scavenger receptors (SRs) are a group of endocytic pattern recognition receptors (PRRs) with ligand-binding activity, which directly bind to proteins, polyribonucleotides, polysaccharides and lipids [1,2]. SRs constitute a large family of proteins that are structurally diverse and participate in a wide range of biological functions, such as fatty acid metabolism, innate immunity, endocytosis of modified lipoproteins, phagocytic clearance of unusable components, like modified host molecules and apoptotic cells, and also pheromone signaling [3–5]. Based on their protein domain architecture and biological function, SRs have been discovered and the definition has been broadened to eight different classes (A-H) in mammals [6].

Scavenger receptors class B (SR-Bs) include scavenger receptor class B type I (SR-BI) (alternative names: SR-B1, SCARB1), SR-BII, cluster determinant 36 (CD36) and lysosomal integral membrane protein 2 (LIMP2) in mammals [7]. All SR-Bs are type III transmembrane receptors with two transmembrane (TM) domains, an extracellular loop with multiple glycosylation sites and two short intracellular tails [8]. SR-BI is a physiologically relevant HDL receptor that mediates selective uptake of lipoprotein (HDL)-derived cholesteryl ester (CE) *in vitro* and *in vivo* [9,10]. SR-BI facilitates the bidirectional flux of free cholesterol (FC) and phospholipids between HDL and cells, thus influencing plasma membrane cholesterol content [11,12]. It has also been implicated in the entry into cells of the hepatitis C virus (HCV) [13–15], protection against female infertility [16], phagocytosis of apoptotic cells [17], plasmodium infection [18,19], chlamydia trachomatis survival in host cells [20], and plays a regulatory role in HDL induced signaling in the vasculature [21,22]. Recent studies of SR-BI showed protection against septic death likely through its role in modulating immune response via TLR4 signaling in macrophages and through its role in removal of LPS from circulation [23]. SR-B1 and LOX-1 participate in BEC activation triggered by the TLR3 ligand dsRNA *in vitro*, and regulate the recruitment of inflammatory cells into the lungs and the activation of T cells and dendritic cells in draining lymph nodes [24]. Furthermore, SR-B1 enhances bacterial adhesion and clinical signs of systemic inflammatory

* Corresponding author.
** Corresponding author.
E-mail addresses: chenkunci@prfri.ac.cn (K. Chen), wangyp@ihb.ac.cn (Y. Wang).

https://doi.org/10.1016/j.fsi.2019.04.031
Received 25 January 2019; Received in revised form 27 March 2019; Accepted 10 April 2019
Available online 13 April 2019

response syndrome in pyometra-affected uteri [25].

SR-BI has been described in many species such as human, mouse [26], shrimp [27,28], and crab [5,29,30], but functional studies on bony fish SR-BI proteins are limited. Kleveland et al. [31] reported that SR-BI has an important function in intestinal lipid absorption in Atlantic salmo (*Salmo salar* L.). Raldúa and Babin [32] pointed out that BLT-1 inhibits SR-BI activity and induces a copper-dependent phenotype during zebrafish (*Danio rerio*) development. Sundvold et al. [33] found a novel paralog of *SCARB1* (*SCARB1-2*) in Atlantic salmon, and thought this gene may be a possible source of genetic variation in salmonid flesh pigmentation. Eslamloo et al. [34] indicated that there is a time-dependent down-regulation for *scarb1-a*, *scarb1-b* and *csf1r* in salmon macrophage-like cells (MLCs) within the polyriboinosinic polyribocytidylic acid (pIC) stimulation at 24 h post-stimulation compared to the earlier time point. Because of the multiple function of SR-B1, it is necessary to conduct studies in bony fishes.

Grass carp (*Ctenopharyngodon idellus*) is a crucial aquaculture species in China, but tremendous economic loss is often caused by Grass Carp Reovirus (GCRV), a dsRNA virus. The genome of GCRV contains 11 segments of linear dsRNA, which encodes seven structural proteins (VP1-VP7) and five nonstructural proteins (NS80, NS38, NS31, NS26, and NS16), respectively. VP1-VP4 and VP6 are the components of the viral core, and the outer GCRV capsid is composed of 200 trimers of VP5 and VP7 heterodimers [35]. It is essential to investigate the pathogenesis of GCRV infection and look for preventative measures to promote sustainable culture of grass carp. However, the bigger size and longer reproductive cycle of the grass carp make it difficult to study the mechanism. The rare minnow (*Gobiocypris rarus*), which is a small cyprinid species, has been recognized as a useful model for aquatic toxicity testing, chemical safety assessments, and antiviral breeding [36]. Also, it is very sensitive to GCRV, and its mortality is 100%.

In our previous study, transcriptome of GCRV-infected *C. idellus* kidney (CIK) cells showed that *srb1*, *itgb2* and sec*22b* appear to be up-regulated during 8–24 h post infection period, which suggest that *itgb2* and/or *srb1* may be important for cell entry of GCRV [37]. In the current study, we employed the rare minnow as a model fish to study the mechanism of GCRV infection. A full-length cDNA sequence encoding SRB1 protein from *G. rarus* was identified and designated as *Gr*SRB1. The expression patterns of *GrSRB1* gene in different healthy tissues were analyzed, and the response to GCRV infection in immune tissues was studied. In addition, the relationship between some major outer capsid proteins of GCRV and *Gr*SRB1 was also investigated. Our findings will help us to better understand fish SRB1 and its potential functions for virus entry into host cells.

2. Materials and methods

2.1. Fish and cell

The five-month-old healthy rare minnows, weighting about 2 ± 0.3 g with an average length of 3 ± 0.5 cm, were raised and maintained under standard laboratory conditions at China Zebrafish Resource Center (CZRC) (http://en.zfish.cn/). Before performing the GCRV challenge experiments, 150 fish were acclimatized in 30 L aerated fresh water at 28 ± 1 °C and fed twice daily with the commercial diet for one week. After no abnormal symptoms were observed, the rare minnows were subjected to further study.

Human embryonic kidney 293T (HEK293T) cells used in the study were obtained from China Center for Type Culture Collection (CCTCC) (http://www.cctcc.org/), and cultured in Dulbecco's modified Eagle's medium (High Glucose) (Gibco, USA) supplemented with 10% (v/v) fetal bovine serum (Gibco, USA) containing penicillin (100 IU/ml) and streptomycin (100 mg/ml) (Hyclone, USA). Cells were maintained at 37 °C in a humidified atmosphere of 5% CO_2.

2.2. GCRV challenge and sampling

Before GCRV challenge, five healthy fish were sacrificed as one group, and samples from the gills (G), liver (L), spleen (S), intestine (I), middle kidney (MK), muscle (M), head kidney (HK), heart (H), and brain (B) were collected. At the same time, fin tissue was obtained and fixed in 95% ethanol. GCRV (GD108 strain) was used for challenge experiments, and the operation was referring to Ou et al. reported [38]. Five individuals were killed and tissues including gills (G), liver (L), spleen (S) and intestine (I) were collected at 0, 6, 12, 18, 24, 48, 72, 96, 120, and 144 h after GCRV exposure. Three groups we collected at each time points. All samples were immediately homogenized in TRIzol reagent (Invitrogen, USA) and stored at −80 °C until RNA extraction.

2.3. RNA extraction and cDNA synthesis

The total RNAs were extracted according to the manufacturer's instruction for TRIzol reagent. Using random hexamer primer (Takara, Japan) and M-MLV Reverse Transcriptase (Promega, USA), first strand cDNA synthesis which used for the fragment amplification were performed on liver-derived RNA; SMART™ RACE cDNA Amplification Kit (Takara, Japan) was used to obtain 5′-RACE Ready cDNA and 3′-RACE Ready cDNA; ReverTra Ace qPCR RT Kit(Toyobo, Japan)was utilized to synthesize cDNA that were used as templates for qRT-PCR.

2.4. Full-length cDNA cloning and sequence analysis for GrSRB1

To identify *GrSRB1* cDNA sequences, primers GrSRB1-F1 and GrSRB1-R1 (Table 1) were designed and synthesized based on the highly conserved regions of known fish *SRB1* sequences including *D. rerio* (*DrSRB1*, Accession no. NM_198921.2), *Oryzias latipes* (*OlSRB1*, Accession no. XM_011481416.2), *Cyprinus carpio* (*CcSRB1*, Accession no. XM_019104218.1), *Salmo salar (SsSRB1,* Accession no. NM_001123612.1), and *Esox lucius* (*ElSRB1*, Accession no. XM_010878228.3). The 3′ untranslated regions (UTRs) were obtained according to the manufacturer's instruction for SMART™ RACE cDNA Amplification Kit. The cDNA sequence was confirmed by sequencing the PCR product amplified by primers GrSRB1-F1 and GrSRB1-R2 (Table 1) within the 3′ UTRs.

Sequences of *GrSRB1* were analyzed using the Sequence Manipulation Suite (STS) (http://www.bio-soft.net/sms/). The BLASTP program (https://blast.ncbi.nlm.nih.gov/Blast.cgi) was used to search for SRB1 protein sequences from other species in the NCBI (http://www.ncbi.nlm.nih.gov/). Multiple sequence alignments were performed by the ClustalX 2.1 program (http://www.ebi.ac.uk/tools/clustalx2.1). Simple Modular Architecture Research Tool (SMART) (http://smart.embl-heidelberg.de/) was used to predict the protein domain features. The NetNglyc 1.0 server (http://www.cbs.dtu.dk/services/NetNGlyc/) predicted the *N*-Glycosylation sites of SRB1. A phylogenetic tree was constructed by the neighbor-joining (NJ) algorithm embedded in Mega 5.0 software (http://www.megasoftware.net/index.html) with a minimum of 1000 bootstraps.

2.5. Cloning the genomic sequence of GrSRB1 gene

Based on the cDNA sequences of *GrSRB1*, primers (Table 2) were designed to amplify the genomic sequences gradually. Genomic DNA (gDNA) was extracted from the tail fin using Universal Genomic DNA Kit (CWBio, China) according to the manufacturer's instructions. Ten pairs of primers worked well, and ten overlapping fragments which covered the full-length cDNA sequence were amplified and sequenced (Table 2). The exons and introns were determined by comparing the gDNA sequences with the cDNA sequences of *GrSRB1* gene.

Table 1
Primers for full-length cDNA cloning and qRT-PCR.

Primer name	Sequence (5'→3')	Application
GrSRB1-F1	ATGGCGGTGTCTAAATCTAC	partial sequence obtaining
GrSRB1-R1	GGACCATCAATGTAGCCG	
GrSCARB-3′F-out	TCAGAAACAGGAAAGATAACGGAGGTG	3′-Race PCR amplification
rSCARB-3′F-in	AGAGAGCGGCTACATTGATGGTCCT	
GrSRB1-F1	ATGGCGGTGTCTAAATCTAC	ORF qualifying
GrSRB1-R2	CACAGCACTTCATAAAATAACTT	
GrSRB1-qF	GCGTCAGTAATGATGGAGAAT	qRT-PCR amplification
GrSRB1-qR	TCCACCAACTTGCTGTCG	
Grβ-actin-qF	TGTAGCCACGCTCGGTCAG	qRT-PCR amplification
Grβ-actin-qR	GGTATCGTGATGGACTCTGGTG	
GrSRB1-MQ-F	CCGGAATTCGGATGAAGAATGTAGAGATAAACCCGA	plasmid construction
GrSRB1-MQ-R	CGGGGTACCTTACACCACCAGATTAGTGCGGA	
VP7-MQ-F	GAAGATCTCTATGCCACTTCACATGATTCCG	plasmid construction
VP7-MQ-R	GCGGCCGCTTAATCGGATGGCTCCACATG	
VP5-MQ-F	GAAGATCTCTATGTGGAACGTTCAAACCTC	plasmid construction
VP5-MQ-R	GCGGCCGCTCACTTGCCGGGCCA	
VP7G-MQ-F	AGACTCGAGGTATGGCCACTCGTGACAGC	plasmid construction
VP7G-MQ-R	GCGGCCGCTGGTTACTTACAGCAAACTACCGTCC	

Table 2
Primers for genomic DNA sequences.

Primer name	Sequence (5'→3')	Length (bp)
GrSRB1-gDNA-F1	ATGGCGGTGTCTAAATCTAC	922 bp
GrSRB1-gDNA-R1	CGTTCTTCGGGTTTATCTC	
GrSRB1-gDNA-F2	AGATAAACCCGAAGAACGAACT	2592 bp
GrSRB1-gDNA-R2	TGACCACATCAGTTTCATCTCC	
GrSRB1-gDNA-F3	TGGTCACCATCCCTAACAT	1035 bp
GrSRB1-gDNA-R3	TGTTCAGGAAGTCCACCAA	
GrSRB1-gDNA-F4	GCGATACCCAACCCTACCAC	459 bp
GrSRB1-gDNA-R4	TCAGGCCATTCCAAGAGTCC	
GrSRB1-gDNA-F5	GCTTATTTGCTGAGGTGGGTGT	1266 bp
GrSRB1-gDNA-R5	CACGCATCAGGGCTGTAGAAG	
GrSRB1-gDNA-F6	AATGTGGATTACTGGAGGTCTGAT	236 bp
GrSRB1-gDNA-R6	CCTCTGGAACACCAGCTCC	
GrSRB1-gDNA-F7	CCTTCTACAGCCCTGATGC	936 bp
GrSRB1-gDNA-R7	GTTGGGAAATGAACACAGG	
GrSRB1-gDNA-F8	TTCCCCTGTGTTCATTTCC	356 bp
GrSRB1-gDNA-R8	TCCGTTATCTTTCCTGTTTCTG	
GrSRB1-gDNA-F9	TCATTAAGAGCGTTTCGGG	737 bp
GrSRB1-gDNA-R9	GGCAGCACCACCAGATTAGT	
GrSRB1-gDNA-F10	AGCGGCTACATTGATGGTCC	2519 bp
GrSRB1-gDNA-R10	TGGGGTCTTTTCACTGGCTG	

2.6. Quantification of gene expression

qRT-PCR was established in a CFX96™ Real-Time PCR Detection System (Bio-Rad, USA) to quantify mRNA expression of *GrSRB1* in different tissues, including gills (G), liver (L), spleen (S), intestine (I), middle kidney (MK), muscle (M), head kidney (HK), heart (H), and brain (B). Specific primers (Table 1) were designed for qRT-PCR. The housekeeping gene *β-actin* was utilized as an internal control for cDNA normalization [39], and the expression level in the gills (G) was used as the baseline (1.0) for qRT-PCR. The relative expression was calculated as the ratio of gene expression in each of the different tissues relative to that in the gills (G). Three replicate qRT-PCR analyses were performed per sample. Expression levels of *GrSRB1* gene were calculated using the $2^{-\triangle\triangle Ct}$ method [40]. The *GrSRB1* expression levels (expressed as mean ± standard deviation) were analyzed by one-way analysis of variance, followed by Dunnett's test for multiple comparisons using SPSS Statistics 20 software. $P < 0.05$ was considered to be statistically significant.

2.7. Temporal expression profiles of GrSRB1 in immune tissues after GCRV challenge

To determine the effects of viral infection on *GrSRB1* mRNA expression in the innate immune system, four representative immune tissues: gills (G), liver (L), spleen (S) and intestine (I), were employed [41]. Fish (five for each time point) were sacrificed at 0, 6, 12, 18, 24, 48, 72, 96, 120, and 144 h post GCRV challenge and tissues were collected for qRT-PCR. The housekeeping gene *β-actin* was used as the reference gene and the expression level of the untreated groups (0 h) was set as the baseline (1.0) for qRT-PCR. The relative expression was calculated as the ratio of gene expression in the treated groups at each time point relative to that in the untreated groups.

2.8. Plasmid construction, transfection, co-immunoprecipitation assay and immunoblot analysis

For GCRV, the outer capsid proteins, such as VP7, VP5 are always proved to play key roles in virus's attachment and infection by interacting with proteins expressed on host cell surface (Cheng et al., 2008; Yan et al., 2015). Some sequences of GCRV were collected from NCBI and synthetized by commercial company (Quintara, China) (*VP5* gene from GCRV-873, Accession no. AF239175.1; *VP7* gene from GCRV-873, Accession no. AF403396.1; *VP7* gene from GCRV-GD108 (designated it as *VP7G* in this paper), Accession no. HQ231203.1). *Bgl* II and *Not* I restriction sites were used to clone *VP5* and *VP7* gene into pCMV-Myc plasmid to construct pCMV-Myc-VP5 and pCMV-Myc-VP7 plasmids, and *Xho* I and *Not* I restriction sites were used to construct pCMV-Myc-VP7G plasmid (specific primers were showed in Table 1). To generate pCMV-HA-*Gr*SRB1, specific primers (Table 1) with *EcoR* I and *Kpn* I restriction sites were used to clone *GrSRB1* gene into pCMV-HA plasmid. pCMV-Myc-VP7, pCMV-Myc-VP5 and pCMV-Myc-VP7G plasmids were co-transfect with pCMV-HA-*Gr*SRB1 plasmid with Lipofectamine® 3000 (Invitrogen, USA) according to the manufacturer's instructions into HEK293T cells, respectively. At the same time, pCMV-Myc-VP7, pCMV-Myc-VP5 and pCMV-Myc-VP7G plasmids were co-transfect with pCMV-HA plasmid, respectively, which were used as controls. Cells were used for co-immunoprecipitation assays after 24 h transfection.

Co-immunoprecipitation assay and immunoblot analysis were conducted as the previously described [41] with slight modifications. For co-immunoprecipitation assays, cells were lysed with RIPA buffer (50 mM Tris-HCl (pH 7.4), 150 mM NaCl, 1% NP-40, 0.1% SDS, 5 mM EDTA) supplemented with protease and phosphatase inhibitors for 20 min at 4 °C. After centrifugation at 12,000 g for 5 min, the supernatant was collected. Total cell lysates (TCL) were incubated with EZ-view™ Red Anti c-Myc Affinity Gel (Sigmal, USA) at 4 °C for 8 h, the bead-bound immune-precipitates (IP) were washed with RIPA buffer five times and stored at −80 °C. For immunoblotting analysis, samples

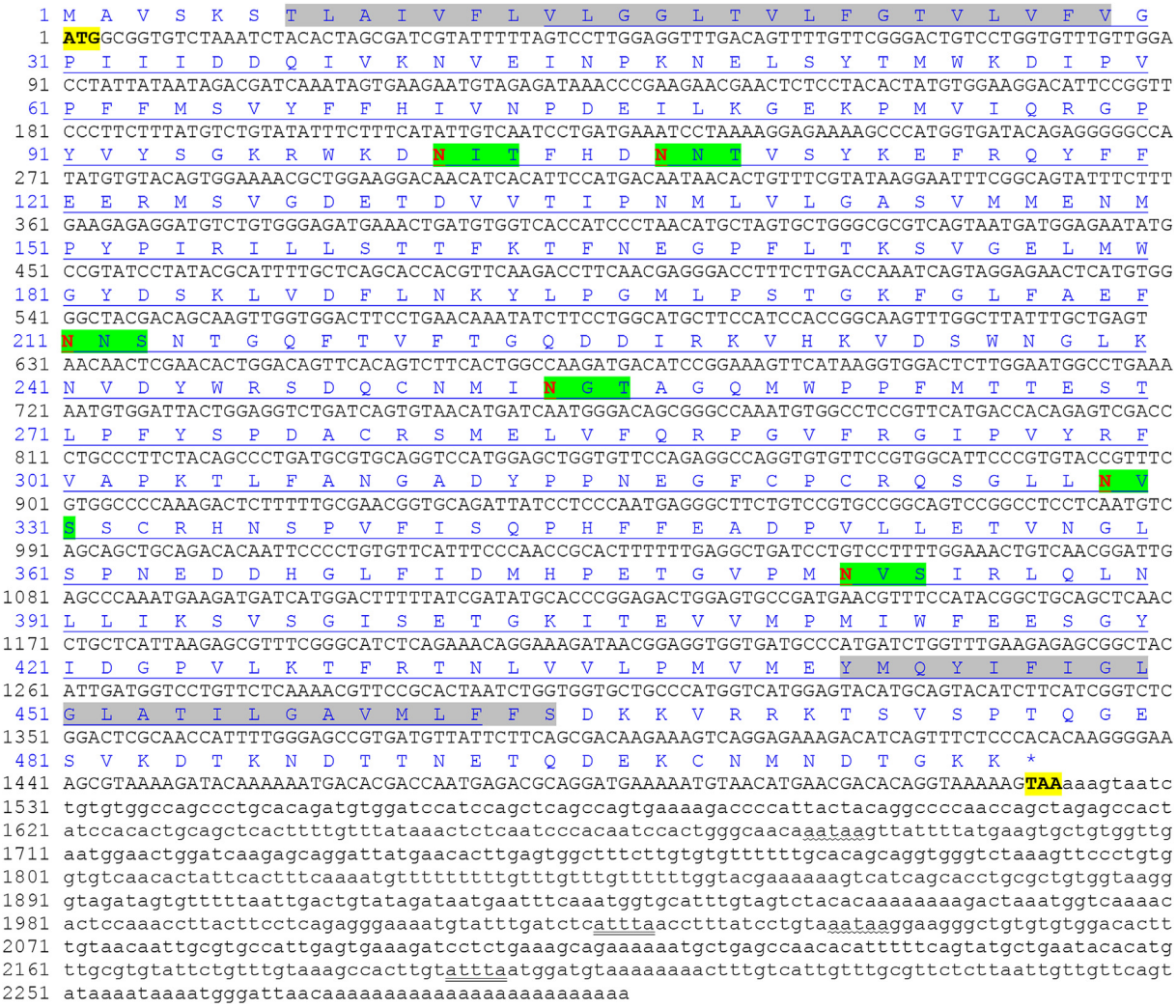

Fig. 1. Nucleotide and putative amino sequences of *Gr*SRB1. The sequences numbers of nucleotide (lower row) and putative amino acid (upper row) are shown on the left. The translation initiation codon (ATG), stop codons (TAA) are in bold and yellow background. The motif associated mRNA instability (ATTTA) is shown as double underscore, and poly-adenylation signal sequence (AATAA) is shown as wavy line. The TM regions are marked with gray background. The CD36 domain are showd as underscore. Asn-Xaa-Ser/Thr sequons in the sequence output below are highlighted in green background, and asparagines predicted to be *N*-linked glycosylation sites are highlighted in bold and in red. (For interpretation of the references to colour in this figure legend, the reader is referred to the Web version of this article.)

were eluted with 6 × SDS loading buffer (Sangon, China) by boiling for 10 min, then resolved by SDS-PAGE and transferred to the PVDF membrane (Millipore, USA). Immunoblots (IB) were visualized using the ECL system (Bio-Rad, USA). The following antibodies were used in immunoblotting analysis: *anti-c*-Myc (1:1000) and anti-HA (1:1000) antibodies were from Sigma (USA), antibody for *anti*-GAPDH (1:1000) was purchased from Santa Cruz Biotechnology (Japan).

3. Results

3.1. Sequences analyses of GrSRB1

The *GrSRB1* cDNA (GenBank Accession no. MK436208) is 2296 bp in length with an ORF of 1521 bp encoding 506 amino acids (aa), 775 bp 3′-UTR with two RNA instability motifs (ATTTA), two poly(A) signal sequences (AATAA) and a poly (A) tail (Fig. 1). *Gr*SRB1 protein was determined to have a CD36 domain (aa 14–462) that shared two transmembrane (TM) regions at the *N*-terminal (aa 7–29) and *C*-terminal (aa 442–464) of the protein. Six putative *N*-linked glycosylation sites (residues 101, 107, 211, 254, 329 and 382) were also predicted in *Gr*SRB1 (Fig. 1).

The genomic sequences of *GrSRB1* was 10792 bp in length, which contained 13 exons and 12 introns following the consensus rule of GT/AG (Fig. 2). Comparison of *SRB1* genomic structures from *C. carpio* (Gene ID: 109090404), *D. rerio* (Gene ID: 387260), *O. latipes* (Gene ID: 100144361), *Homo sapiens* (Gene ID: 949), *Mus musculus* (Gene ID: 20778), *Bos Taurus* (Gene ID: 282346), *Xenopus tropicalis* (Gene ID: 100490714) and *Gallus gallus* (Gene ID: 416814) demonstrated that the genomic structure of *GrSRB1* was same with *CcSRB1* that composed of 13 exons and 12 introns (Fig. 2). There were variations in the number of exons and introns in different species, for example, genome of *DrSRB1*, *HsSRB1*, *BtSRB1*, *XtSRB1* and *GgSRB1* contained 12 exons, while *OlSRB1* contained 14 exons and *MmSRB1* only contained 11 exons.

The lengths of most CDS sequence were conserved, and the lengths of the second to sixth exons were conservative. Notably, the size of *GrSRB1* genomic sequence was smaller than those of other species and the differences in length mainly resulted from various length in introns.

3.2. Multiple alignments and phylogenetic analysis

BLASTP analysis (Fig. 3) showed that *Gr*SRB1 had highest similarity to *Cc*SRB1 (81.85%) and *Dr*SRB1 (79.84%), while the lowest similarity

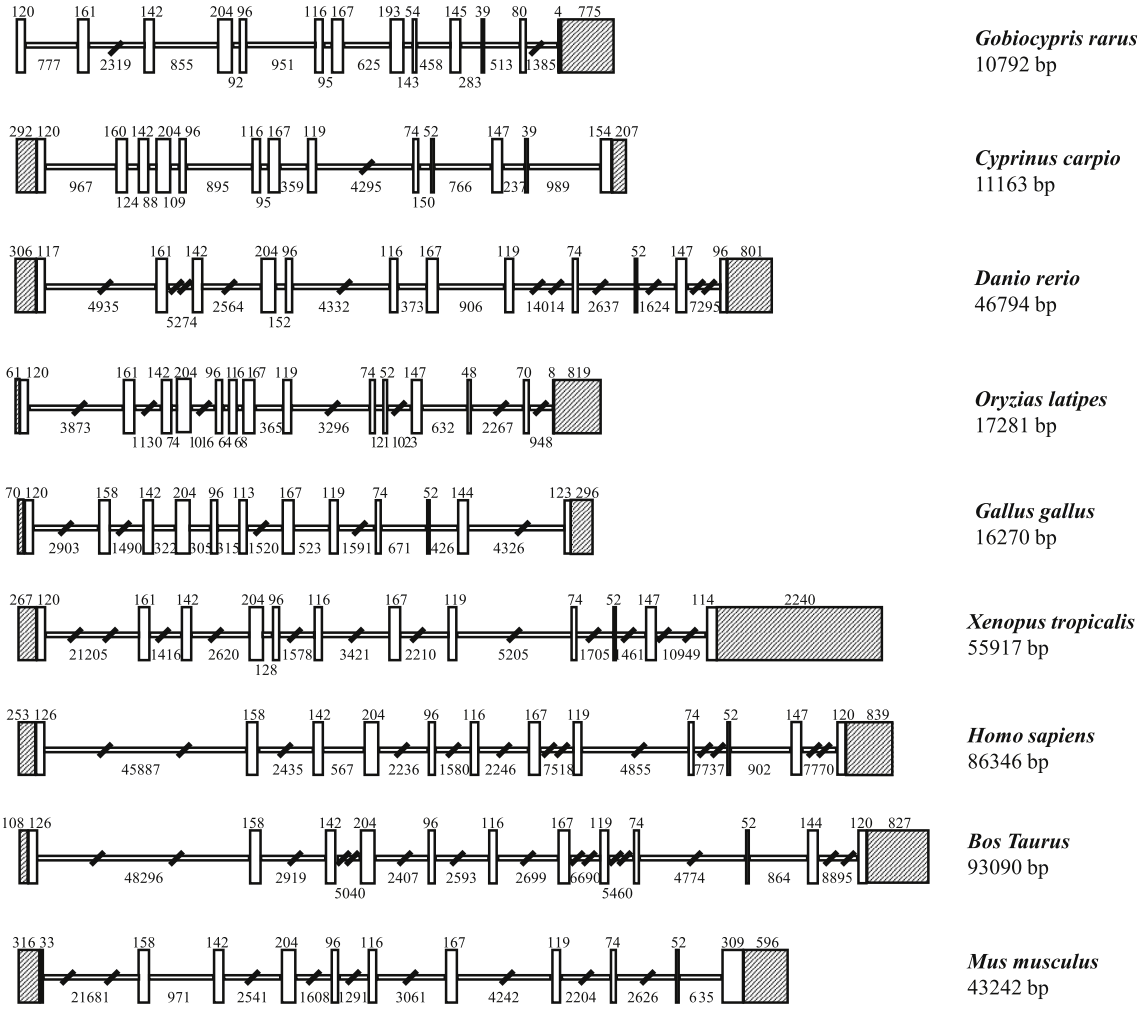

Fig. 2. Genomic structure of *SRB1* genes. The lengths of the elements are shown in base pairs (bp), and the numbers above and below each schematic represent the lengths of exons and introns of corresponding gene, respectively.

to *Mm*SRB1 (46.63%). Besides, *Gr*SRB1 had the sequence similarities with *Ol*SRB1 (69.43%), *Gg*SRB1 (53.16%), *Xt*SRB1 (51.98%), *Hs*SRB1 (51.18%), and *Bt*SRB1 (49.80%), respectively.

Phylogenetic analysis further supported the sequence similarity (Fig. 4). Homologous amino acid sequences from other teleost fish and non-fish were gained from NBCI to construct phylogenetic tree. According to the phylogenetic tree, these homolog proteins could be divided into five groups, consisting of mammals, birds, amphibians, fishes and invertebrates. All the fish SRB1 proteins clustered together, and diverged from their counterparts in other species, such as *H. sapiens*, *B. taurus*, *M. musculus*, *G. gallus*, and *X. tropicalis*. SRB1 proteins in invertebrates were far separated from SRB1 proteins in vertebrates. The phylogenetic tree reflected it was consistent between the genetic relationship with the evolution of species.

3.3. Tissue distribution of GrSRB1 gene in health fish

qRT-PCR was performed to analyze the tissue distribution of *GrSRB1* mRNA expression. As shown in Fig. 5, *GrSRB1* expression was detected in all tissues tested, and the data were calibrated against expression level in gills (G) with the lowest expression. *GrSRB1* had the highest expression in the liver (L) (18.97 folds, $p < 0.01$); and intermediate levels in the spleen (S) (6.83 folds, $p < 0.01$), intestines (I) (6.04 folds, $p < 0.01$), brain (B) (4.66 folds, $p < 0.01$), muscle (M) (4.55 folds, $p < 0.01$); low levels in the heart (H) (1.67 folds), middle kidney (MK) (1.24 folds), head kidney (HK) (1.20 folds).

3.4. Expression profiles of GrSRB1 gene after GCRV challenge

To determine the effects of viral infection on *GrSRB1* gene expression in the innate immune system, the levels of *GrSRB1* mRNAs in gills (G), liver (L), spleen (S), and intestine (I) tissues were examined. In gills (G), transcription of *GrSRB1* (Fig. 6A) was gradually up-regulated after GCRV challenge, and reached to the peak (5.02 folds, $p < 0.01$) at 72 h, then decreased at 96 h, next it rose to a small peak (2.76 folds, $p < 0.01$) at 120 h and kept this level at 144 h. In liver (L), *GrSRB1* expression (Fig. 6B) gradually increased and arrived at the highest level (9.66 folds, $p < 0.01$) at 24 h, followed by significant gradual decline at 48, 72 and 96 h, subsequently increased another peak at 120 h (4.23 folds, $p < 0.01$), next it declined again at 144 h (2.58 folds, $p < 0.01$). In the spleen (S), the expression level of *GrSRB1* (Fig. 6C) fluctuated and reached a peak (5.81 folds, $p < 0.01$) at 72 h, followed by a drastic decline to the initial level at 96 h, then raised up again at 120 h (2.78 folds, $p < 0.01$), and the significant change could be observed till 144 h (2.02 folds, $p < 0.01$). In the intestine (I), the mRNA expression of *GrSRB1* (Fig. 6D) was up-regulated after GCRV infection and peaked at 18 h (4.17 folds, $p < 0.01$), following a down-regulation and reached the lowest level at 72 h (0.74 folds, $p < 0.05$), subsequently the expression of *GrSRB1* exhibited unstable changes and returned to the original level at 144 h.

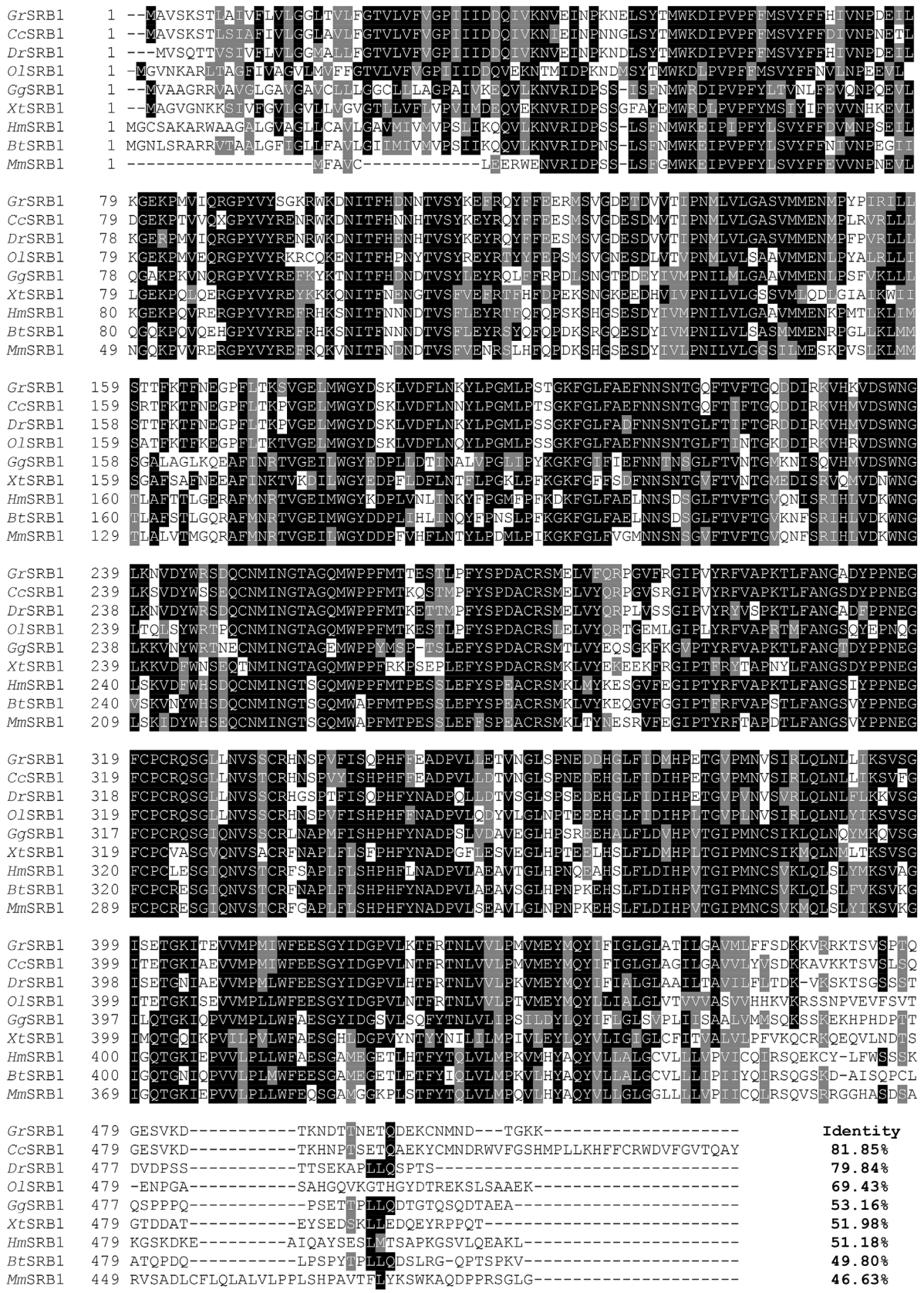

Fig. 3. Multiple alignments of *Gr*SRB1 with SRB1 proteins from various species. The amino acid sequences of SRB1s from typical organisms were aligned using the ClustalW 2.1 program. The black shade represent 100% identity, dark gray represented 80% identity. *Gr*SRB1 stands for SRB1 protein in *G. rarus*, *Cc*SRB1 stands for SRB1 protein in *C. carpio* (Protein ID. XP_018959763.1), *Dr*SRB1 stands for SRB1 protein in *D. rerio* (Protein ID. NP_944603.2), *Ol*SRB1 stands for SRB1 protein in *O. latipes* (Protein ID. XP_011479718.1), *Gg*SRB1 stands for SRB1 protein in *G. gallus* (Protein ID. XP_415106.2), *Xt*SRB1 stands for SRB1 protein in *X. tropicalis* (Protein ID. XP_004910599.1), *Hs*SRB1 stands for SRB1 protein in *H. sapiens* (Protein ID. NP_005496.4), *Bt*SRB1 stands for SRB1 protein in *B. taurus* (Protein ID. XP_005217795.1), *Mm*SRB1 stands for SRB1 protein in *M. musculus* (Protein ID. XP_017176253.1).

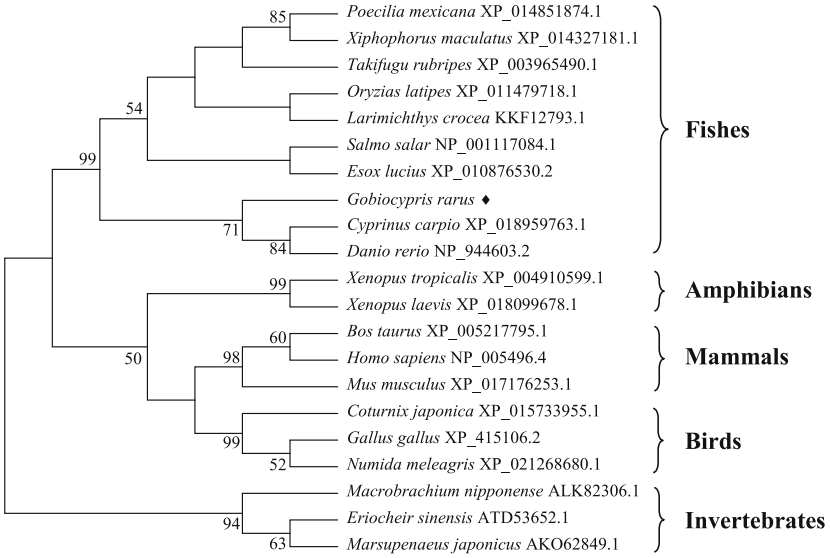

Fig. 4. Phylogenetic relationship between the SRB1 proteins in different species. A neighbor-joining phylogenetic tree was constructed using MEGA 5.0 software. The bootstrap values of the branches were obtained by testing the tree 1000 times and values were over 50% percent marked. The GenBank accession numbers of SRB1 proteins are given after the species names in the tree.

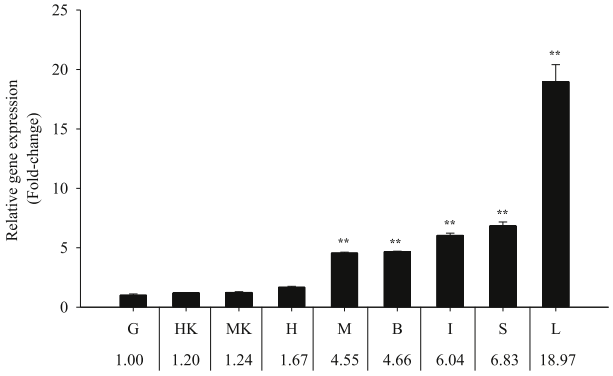

Fig. 5. qRT-PCR analysis of the distribution of *GrSRB1* in different tissues of rare minnows. Expression of *β-actin* was used as an internal control for qRT-PCR. The relative expression was the ratio of gene expression in different tissues relative to that in the gills (G). Detailed values are listed at the bottom of the figure. The assay was performed three times, and data were analyzed by the unpaired *t*-test. $^{**}p < 0.01$, compared with control.

3.5. GrSRB1 specifically interacts with GCRV proteins

To address the mechanism of SRB1 action, testing whether it is receptor of GCRV, we explored whether *Gr*SRB1 could interact with VP5 and VP7 proteins from GCRV-873 strain, VP7G protein from GCRV-GD108. *In vitro*, the transient transfection and co-immunoprecipitation assays revealed that *Gr*SRB1 could interacted with all of the tested outer GCRV proteins. Moreover, the results showed that *Gr*SRB1 had a different affinity for these virus proteins, which had the highest affinity with VP7G protein from GCRV-GD108 (Fig. 7). These data suggest that *Gr*SRB1 might play a vital role in the cell entry of GCRV.

4. Discussion

To date, the mechanism of GCRV entry into host cells remains poorly understood. It is important to note that many viruses use SR-BI as receptors for entry into host cells. In the case of HCV infection, SR-BI is an essential factor for HCV entry into infected cells and such an interaction is mediated by ApoB-containing lipoproteins that are associated with HCV [42,43]. In the case of dengue virus (DV) infection, ApoA-I is associated with DV, and its interaction with cell surface receptor SR-BI could bring DV to cells, which facilitates virus attachment and entry [44]. Moreover, SR-B1 and LOX-1 might serve as co-receptors for TLR3 and act as carriers, facilitating dsRNA entry and delivery to the dsRNA-sensing receptors in bronchial epithelial cells (BEC). As a result, these receptors recognize danger signals associated with lytic virus infections [24]. However, in teleost fish, the role of SRB1 in virus infection remains unclear. In our previous study, transcriptome of GCRV-infected CIK cells indicated that *srb1* may be important for cell entry of GCRV [37].

SR-B1 are highly structural conserved from *Eriocheir sinensis* to humans, all of them include a CD36 domain, two transmembrane regions, and cytoplasmic tails at their *N*-terminus and *C*-terminus [6]. Functionally, the CD36 domain is responsible for ligand binding, and the cytoplasmic tails are thought to be involved in signal translocation. In our results, a cDNA from *G. rarus,* homolog of *SRB1* has been identified and designated as *GrSRB1*. Similarly, the predicted domains of *Gr*SRB1 also contain an extracellular domain, two transmembrane regions and two cytoplasmic tails. There are many structural similarities between fish and mammalian SR-BI, and hence it is likely that SR-BI is also functionally conserved phylogenetically. In mammals, the organ distribution of SR-BI are predominantly expressed in tissues with significant roles in cholesterol metabolism, namely the liver and steroidogenic tissues [7]. Moreover, SR-BI are abundantly expressed in phagocytic cells such as mature monocytes, macrophages, dendritic cells, and neutrophils [45]. In teleost fish, Atlantic salmon *SR-BI* was found a particularly high mRNA expression in midgut [31]. Sundvold et al. [33] found a novel paralog of *SCARB1* in Atlantic salmon, and the *SCARB1-2* mRNA level in muscle equals its expression in liver and mid gut. In this study, the tissue distribution of *GrSRB1* revealed that it has highest mRNA expression level in liver (L), and relatively high expression in intestine (I) and spleen (S). Our results are consistent with those in mammals and other fish.

Transcriptome of GCRV-infected CIK cells showed that *srb1* appeared to be up-regulated during the 8–24 h post infection period, which is closely related to autophagy of host cells [37]. In order to known whether SRB1 plays important role in cell entry of GCRV, the mRNA expression analysis of the *GrSRB1* gene was performed in the immune tissues of the gills (G), liver (L), spleen (S), and intestine (I) after GCRV challenge. In general, the expression level of *GrSRB1* gene showed a consistent change trend in these tissues after GCRV infection, which increased at first and then decreased after reaching the peak. Fig. 6A showed that the expression of *GrSRB1* reached the peak at 72 h in gills; *GrSRB1* expression arrived at the highest level at 24 h in liver (Fig. 6B); in the spleen (S), the expression level of *GrSRB1* reached a peak at 72 h (Fig. 6C); in the intestine (I), the mRNA expression of *GrSRB1* peaked at 18 h (Fig. 6D). The intestines are the first organ for

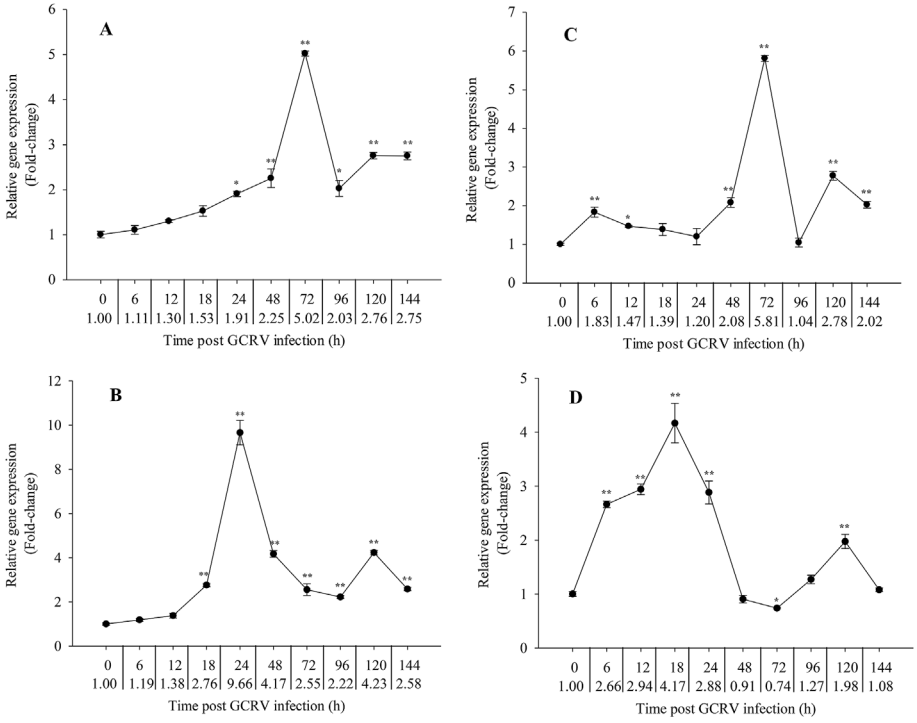

Fig. 6. mRNA expression profiles of *GrSRB1* in immune tissues at different time points following GCRV challenge. The mRNA level in the gills (G) (A), liver (L) (B), spleen (S) (C), and intestine (I) (D) at 0 h-144 h post-infection were subjected to a qRT-PCR analysis. The expression of the *GrSRB1* in the untreated groups (0 h) was set as 1.0. *β-Actin* was used as the internal control to normalize the relative expression level of the target gene. Error bars indicate standard deviation. Detailed values are listed at the bottom of the figure. $*p < 0.05$, $**p < 0.01$, compared with control.

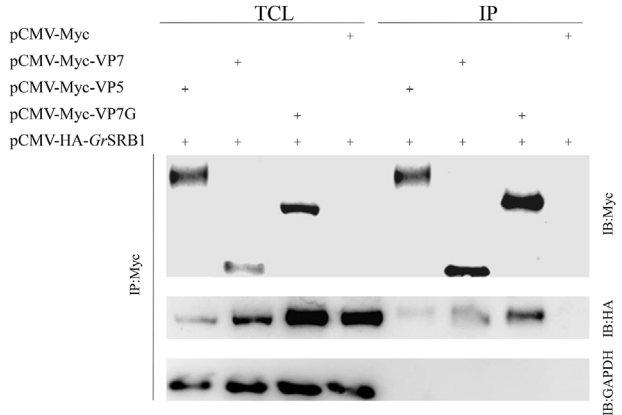

Fig. 7. *Gr*SRB1 interacts with GCRV proteins in mammalian over-expression system. The HEK293T cells (2×10^6) were transfected with the indicated plasmids (5 μg each) for 24 h before co-immunoprecipitation assay and immunoblot analysis were performed with the indicated antibodies. TCL: total cell lysate; IP: immunoprecipitation analysis; IB: immunoblotting analysis.

GCRV entering into the gut, which are continually exposed to a wide range of antigens and potential immune stimuli, they are also the organs that exhibit the symptom of bleeding during GCRV infection. Thus, the expression levels of GrSRB1 in intestines showed an upward trend at early time after GCRV challenge. The up-regulation of *GrSRB1* expression in those immune tissues during the early infection period may be facilitate the entry of GCRV into host cells.

Studies on the characteristics of infectious GCRV particles have demonstrated that complete digestion of VP7 and partial cleavage of VP5 can lead to enhanced infectivity of the virus, indicating that VP7 and VP5 may play very important roles in GCRV entry into host cells during infection [35,46]. Usually, the initial step in a successful viral infection cycle includes the specific binding of a viral structural protein with cellular receptors expressed on the surface. Thus, to determine if SRB1 is the factor that is associated with GCRV and promotes virus infection, we explored the relationship between *Gr*SRB1 protein and the outer capsid protein of GCRV (VP5 and VP7) by co-immunoprecipitation *in vitro*. Fig. 7 revealed that *Gr*SRB1 could interacted with VP5 and VP7 proteins from GCRV-873 strain, VP7G protein from GCRV-GD108. For efficient cell entry, animal viruses engage several different routes to initiate infection. The endocytic pathways are known to be major mechanisms for most animal virus entering host cells. Previous research indicated that endocytosis plays an important role in GCRV entry, while different GCRV isolates may be adopt different endocytic pathways. Wang et al. [47] reported that GCRV-JX01 might enter CIK cells via clathrin-mediated endocytosis in a pH-dependent manner; Zhang et al. [48] pointed that GCRV-873 can use caveolae/raft-mediated endocytosis as the primary entry pathway to initiate productive infection. Our research preliminary suggest that *Gr*SRB1 is associated with GCRV and could bring GCRV to cells, which facilitates virus attachment and entry. However, the specific biological functions of *Gr*SRB1 in endocytic pathways for cell entry require further investigation.

In summary, *Gr*SRB1 was found to have similar expression patterns and similar functions to mammalian SR-B1, and the results of this study indicate that *Gr*SRB1 could be a receptor for GCRV.

Acknowledgments

This work was funded by the Central Public-interest Scientific Institution Basal Research Fund, CAFS [grant number 2018HY-XKQ02-06], National Natural Science Foundation of China [grant number 31572614], and the China Agricultural Research System [grant number CARS-46].

References

[1] T. Areschoug, S. Gordon, Scavenger receptors: role in innate immunity andmicrobial pathogensis, Cell Microbiol. 11 (2009) 1160–1169.
[2] A.M. Pauwels, M. Trost, R. Beyaert, E. Hoffmann, Patterns, receptors, and signals: regulation of phagosome maturation, Trends Immunol. 38 (2017) 407–422.
[3] S. Mukhopadhyay, S. Gordon, The role of scavenger receptors in pathogen recognition and innate immunity, Immunobiology 209 (2004) 39–49.
[4] D.T. MacLeod, T. Nakatsuji, Z. Wang, A. di Nardo, R.L. Gallo, Vaccinia virusbinds to the scavenger receptor MARCO on the surface of keratinocytes, J. Investig. Dermatol. 135 (2015) 142–150.
[5] T. Kong, Y. Gong, Y. Liu, X. Wen, N.T. Tran, J.J. Aweya, et al., Scavenger receptor B

promotes bacteria clearance by enhancing phagocytosis and attenuates white spot syndrome virus proliferation in Scylla paramamosian, Fish Shellfish Immunol. 78 (2018) 79–90.
[6] J. Canton, D. Neculai, S. Grinstein, Scavenger receptors in homeostasis and immunity, Nat. Rev. Immunol. 13 (2013) 621–634.
[7] M. Prabhudas, D. Bowdish, K. Drickamer, M. Febbraio, J. Herz, L. Kobzik, et al., Standardizing scavenger receptor nomenclature, J. Immunol. 192 (2014) 1997–2006.
[8] I.A. Zani, S.L. Stephen, N.A. Mughal, D. Russell, S. Homer-Vanniasinkam, S.B. Wheatcroft, et al., Scavenger receptor structure and function in health and disease, Cells 4 (2015) 178–201.
[9] S. Acton, A. Rigotti, K.T. Landschultz, S. Xu, H.H. Hobbs, M. Krieger, Identification of scavenger receptor SR-BI as a high density lipoprotein receptor, Science 271 (1996) 518–520.
[10] S. Azhar, S. Leers-Sucheta, E. Reaven, Cholesterol uptake is adrenal and gonadal tissues: the SR-BI and 'selective' pathway connection, Front. Biosci. 8 (2003) s998–1029.
[11] A. Rigotti, S.L. Acton, M. Krieger, The class B scavenger receptors SR-BI and CD36 are receptors for anionic phospholipids, J. Biol. Chem. 270 (1995) 16221–16224.
[12] S. Saddar, V. Carriere, W.R. Lee, K. Tanigaki, I.S. Yuhanna, S. Parathath, et al., Scavenger receptor class B type I is a plasma membrane cholesterol sensor, Circ. Res. 112 (2013) 140–151.
[13] E. Scarselli, H. Ansuini, R. Cerino, R.M. Roccasecca, S. Acali, G. Filocamo, et al., The human scavenger receptor class B type I is a novel candidate receptor for the hepatitis C virus, EMBO J. 21 (2002) 5017–5025.
[14] M.T. Catanese, H. Ansuini, R. Graziani, T. Huby, M. Moreau, J.K. Ball, et al., Role of scavenger receptor class B Type I in hepatitis C virus entry: kinetics and molecular determinants, J. Virol. 84 (2010) 34–43.
[15] S. Westhaus, M. Deest, A.T.X. Nguyen, F. Stanke, D. Heckl, R. Costa, et al., Scavenger receptor class B member 1 (SCARB1) variants modulate hepatitis C virus replication cycle and viral load, J. Hepatol. 67 (2017) 237–245.
[16] H.E. Miettinen, H. Rayburn, M. Krieger, Abnormal lipoprotein metabolism and reversible female infertility in HDL receptor (SR-BI)-deficient mice, J. Clin. Investig. 108 (2001) 1717–1722.
[17] Y. Osada, T. Sunatani, I.S. Kim, Y. Nakanishi, A. Shiratsuchi, Signalling pathway involving GULP, MAPK and Rac 1 for SR-BI-induced phagocytosis of apoptotic cells, J. Biochem. 145 (2009) 387–394.
[18] S. Yalaoui, T. Huby, J.F. Franetich, A. Gego, A. Rametti, M. Moreau, et al., Scavenger receptor BI boosts hepatocyte permissiveness to Plasmodium infection, Cell Host Microbe 4 (2008) 283–292.
[19] A.C. Langlois, M. Carine, G. Manzoni, O. Silvie, Plasmodium sporozoites can invade hepatocytic cells independently of the Ephrin receptor A2, PLoS One 13 (2018) e0200032.
[20] J.V. Cox, N. Naher, Y.M. Abdelrahman, R.J. Belland, Host HDL biogenesis machinery isrecruited to the inclusion of Chlamydia trachomatis-infected cells and regulates chlamydial growth, Cell Microbiol. 14 (2012) 1497–1512.
[21] A. Al-Jarallah, B.L. Trigatti, A role for the scavenger receptor, class B type I in high density lipoprotein dependent activation of cellular signaling pathways, Biochim. Biophys. Acta 1801 (2010) 1239–1248.
[22] W.J. Shen, J. Hu, Z. Hu, F.B. Kraemer, S. Azhar, Scavenger receptor class B type I (SR-BI): a versatile receptor with multiple functions and actions, Metabolism 63 (2014) 875–886.
[23] L. Guo, Z. Song, M. Li, Q. Wu, D. Wang, H. Feng, et al., Scavenger receptor BI protects against septic death through its role in modulating inflammatory response, J. Biol. Chem. 284 (2009) 19826–19834.
[24] A. Dieudonné, D. Torres, S. Blanchard, S. Taront, P. Jeannin, Y. Delneste, et al., Scavenger receptors in human airway epithelial cells: role in response to double-stranded RNA, PLoS One 7 (2012) e41952.
[25] C. Gabriel, A. Becher-Deichsel, J. Hlavaty, G. Mair, I. Walter, The physiological expression of scavenger receptor SR-B1 in canine endometrial and placental epithelial cells and its potential involvement in pathogenesis of pyometra, Theriogenology 85 (2016) 1599–1609.
[26] L. Cai, A. Ji, F.C. de Beer, L.R. Tannock, D.R. van der Westhuyzen, SR-BI protects against endotoxemia in mice through its roles in glucocorticoid production and hepatic clearance, J. Clin. Investig. 118 (2008) 364–375.
[27] W.J. Bi, D.X. Li, Y.H. Xu, S. Xu, J. Li, X.F. Zhao, et al., Scavenger receptor B protects shrimp from bacteria by enhancing phagocytosis and regulating expression of antimicrobial peptides, Dev. Comp. Immunol. 51 (2015) 10–21.
[28] Z. Ding, N. Luo, Y. Kong, J. Li, Y. Zhang, F. Cao, et al., Scavenger receptor class B, type I, a CD36 related protein in *Macrobrachium nipponense*: characterization, RNA interference, and expression analysis with different dietary lipid sources, Int. J. Genomics 2016 (2016) 6325927.
[29] N. Yang, D.F. Zhang, Z. Tao, M. Li, S.M. Zhou, G.L. Wang, Identification of a novel class B scavenger receptor homologue in *Portunus trituberculatus*: molecular cloning and microbial ligand binding, Fish Shellfish Immunol. 58 (2016) 73–81.
[30] Y.M. Wu, L. Yang, X.J. Li, L. Li, Q. Wang, W.W. Li, A class B scavenger receptor from Eriocheir sinensis (EsSR-B1) restricts bacteria proliferation by promoting phagocytosis, Fish Shellfish Immunol. 70 (2017) 426–436.
[31] E.J. Kleveland, B.L. Syvertsen, B. Ruyter, A. Vegusdal, S.M. Jørgensen, T. Gjøen, Characterization of scavenger receptor class B, type I in Atlantic salmon (*Salmo salar* L.), Lipids 41 (2006) 1017–1027.
[32] D. Raldúa, P.J. Babin, BLT-1, a specific inhibitor of the HDL receptor SR-BI, induces a copper-dependent phenotype during zebrafish development, Toxicol. Lett. 175 (2007) 1–7.
[33] H. Sundvold, H. Helgeland, M. Baranski, S.W. Omholt, D.I. Våge, Characterisation of a novel paralog of scavenger receptor class B member I (SCARB1) in Atlantic salmon (*Salmo salar*), BMC Genet. 12 (2011) 52.
[34] K. Eslamloo, X. Xue, J.R. Hall, N.C. Smith, A. Caballero-Solares, C.C. Parrish, et al., Transcriptome profiling of antiviral immune and dietary fatty acid dependent responses of Atlantic salmon macrophage-like cells, BMC Genomics 18 (2017) 706.
[35] L. Cheng, Q. Fang, S. Shah, I.C. Atanasov, Z.H. Zhou, Subnanometer-resolution structures of the grass carp reovirus core and virion, J. Mol. Biol. 382 (2008) 213–222.
[36] T. Wang, P. Liu, H. Chen, H. Liu, Y. Yi, W. Guo, Preliminary study on the susceptibility of Gobiocyprisrarus to hemorrhagic virus of grass carp (GCHV), Acta Hydrobiol. Sin. 18 (1994) 144–149 (In Chinese, English abstract).
[37] G. Chen, L. He, L. Luo, R. Huang, L. Liao, Y. Li, et al., Transcriptomics sequencing provides insights into understanding the mechanism of grass carp reovirus infection, Int. J. Mol. Sci. 19 (2018) 488.
[38] M. Ou, R. Huang, L. Xiong, L. Luo, G. Chen, L. Liao, et al., Molecular cloning of the MARCH family in grass carp (*Ctenopharyngodon idellus*) and their response to grass carp reovirus challenge, Fish Shellfish Immunol. 63 (2017) 480–490.
[39] Q. Fang, L. Wang, S. Liu, Z. Wang, Characterization of reference genes in rare minnow, *Gobiocypris rarus* (Actinopterygii: Cypriniformes: Cyprinidae), in early postembryonic development and in response to EDCs treatment, Acta Ichthyol. Piscatoria T. 43 (2013) 127–138.
[40] K.J. Livak, T.D. Schmittgen, Analysis of relative gene expression data using real-time quantitative PCR and the $2^{-\Delta\Delta C}$T method, Methods 25 (2001) 402–408.
[41] B. Van de Kooij, I. Verbrugge, E. de Vries, M. Gijsen, V. Montserrat, C. Maas, et al., Ubiquitination by the membrane-associated RING-CH-8 (MARCH-8) ligase controls steady-state cell surface expression of tumor necrosis factor-related apoptosis inducing ligand (TRAIL) receptor 1, J. Biol. Chem. 288 (2013) 6617–6628.
[42] P. Maillard, T. Huby, U. Andréo, M. Moreau, J. Chapman, A. Budkowska, The interaction of natural hepatitis C virus with human scavenger receptor SR-BI/Cla1 is mediated by ApoB-containing lipoproteins, FASEB J. 20 (2006) 735–737.
[43] R. Harada, M. Kimura, Y. Sato, T. Taniguchi, T. Tomonari, T. Tanaka, et al., APOB codon 4311 polymorphism is associated with hepatitis C virus infection through altered lipid metabolism, BMC Gastroenterol. 18 (2018) 24.
[44] Y. Li, C. Kakinami, Q. Li, B. Yang, H. Li, Human apolipoprotein A-I is associated with dengue virus and enhances virus infection through SR-BI, PLoS One 8 (2013) e70390.
[45] I.N. Baranova, T.G. Vishnyakova, A.V. Bocharov, A. Leelahavanichkul, R. Kurlander, Z. Chen, et al., Class B scavenger receptor types I and II and CD36 mediate bacterial recognition and proinflammatory signaling induced by Escherichia coli, lipopolysaccharide, and cytosolic chaperonin 60, J. Immunol. 188 (2012) 1371–1380.
[46] S. Yan, J. Zhang, H. Guo, L. Yan, Q. Chen, F. Zhang, et al., VP5 autocleavage is required for efficient infection by in vitro-recoated aquareovirus particles, J. Gen. Virol. 96 (2015) 1795–1800.
[47] H. Wang, W. Liu, F. Yu, L. Lu, Disruption of clathrin-dependent trafficking results in the failure of grass carp reovirus cellular entry, Virol. J. 13 (2016) 1–10.
[48] F. Zhang, H. Guo, J. Zhang, Q. Chen, Q. Fang, Identification of the caveolae/raft-mediated endocytosis as the primary entry pathway for aquareovirus, Virology 513 (2018) 195–207.